Review Article

Oni Olubukola Aina*, Ahzegbobor P. Aizebeokhai, and Boyo Henry Oritsemamididasan

Analysis of aeromagnetic filtering techniques in locating the primary target in sedimentary terrain: A review

https://doi.org/10.1515/phys-2021-0045
received March 31, 2021; accepted May 21, 2021

Abstract: This article analyzes some aeromagnetic filtering techniques for mitigating deceptive geophysical conceptions that may result in a distorted range of geological information from aeromagnetic data. The implication of using the aeromagnetic method, data processing, and enhancement to distinguish sediment-produced anomalies was considered. Two methods to locate buried faults in aeromagnetic data were compared: Edge and fault detection were considered using the magnetic contrast and horizontal gradient methods, whereas rapid depth estimation was considered using the Euler deconvolution method and Signum method. The general challenge to find the magnetic anomaly depth and delineate edges relies on geophysical filtering techniques discussed in order to maintain its geological relevance. The magnetic-contrast layer model signatures help clarify the existence of intra-sedimentary faults. The horizontal gradient approach relative to other derivative methods has better noise stability and fast adaptation to grids without modifying parameters. However, the Signum transform (ST) approach offers a more special solution in depth estimation than the Euler's deconvolution approach whose solution relies on the required choice of default shape parameters and windows. The Euler deconvolution procedure may not be able to detect structures found by the ST approach and *vice versa*. As a result, these techniques may be used in conjunction with one another during analysis, as complementary interpretation tools. This review will however aid in the analysis of information used as a criterion for determining faults using various analytical techniques like ST or Euler deconvolution.

Keywords: aeromagnetic, magnetic-contrast, Euler deconvolution, Signum transform, geophysical techniques

1 Introduction

The aeromagnetic method is focused primarily on the measurement of the magnetic effect created by differing concentrations of ferromagnetic materials, such as magnetite, in geological structures, which is used to extract information relating to direction, the gradient of magnetization, or the Earth's magnetic field intensity [1]. The total magnetic field and or the vertical gradient is usually measured. The measurement of the magnetic field's horizontal or vertical component or horizontal gradient can also be deduced. In order to delineate and estimate the depth of subsurface structures such as faults, dykes, and fractures and to map geological characteristics, analysis and interpretation of aeromagnetic information are essential [2]. These characteristics are displayed in colorful geological contour maps, which, if the limitations of the geophysical method are overlooked, may laterally be interpreted as true characteristics [3].

However, during analysis and interpretation, the variability that controls the varying shapes of an anomaly in geophysical models is as follows:

- Lateral magnetic contrast
- Distance covered by the contrast boundary
- Vertical extent or the dip
- Observation in flight height
- Contact depth from the Earth's surface
- The direction of the magnetization vector.

Therefore, the primary focus of this research is the use of aeromagnetic techniques for the detailed identification of shallow subsurface contact lineages. This article would help in the interpretation of details used as a basis

* **Corresponding author: Oni Olubukola Aina,** Department of Physics, Covenant University, P.M.B 1023, Ota, Ogun State, Nigeria, e-mail: ejiwunmiejiwunmi@gmail.com
Ahzegbobor P. Aizebeokhai: Department of Physics, Covenant University, P.M.B 1023, Ota, Ogun State, Nigeria
Boyo Henry Oritsemamididasan: Department of Physics, Elizade University, Ilara-Mokin, Ondo, Nigeria

for deciding fault using various analytical techniques such as the ST or Euler deconvolution. The concept used in this study is to review aeromagnetic processing methods in order to lessen some misleading geophysical conceptions during data analysis and processing (*e.g.*, incorrect choice of structural index (SI) value can make Euler deconvolution prone to misleading interpretation) if some guidelines described in this review are adhered to.

A review from previous studies shows that the Euler deconvolution technique was used to determine the sedimentary thickness and depth to magnetic source at Northern Bida Basin, Nigeria. The total magnetic intensity (TMI) of magnetic data was reduced to the equator (RTE) grid and a polynomial filter was added to the RTE grid for the separation of regional residual. The Euler depth evaluation for magnetic anomalies and basement rock varied from 3.083 to 12.6 m using Euler deconvolution [4]. Osinowo *et al.* inferred that sedimentary rocks with a low magnetic response dominated the southwestern region, and intra-sedimentary intrusions are the most possible source of other high magnetic effects, which support the presence of oolitic/iron ore or ferruginous sand stone in the region. In another study, Gaussian filter and Reduced to Pole at Low Latitude aeromagnetic data were generated from susceptibility and Analytic Signal (AS) maps and were used to distinguish crystalline basement rocks from sedimentary units [5]. The grids of tilt derivative and its horizontal components at various upward continuation distances were used to delineate shallow (900–1,600 m) sedimentary structures and deeper (1.5–43 km) crustal intra-geologic linear structures. The depth of a potential field from the magnetic source was estimated using the Euler deconvolution depth weighting method based on Hilbert transform equations, which use a magnetic field and its three orthogonal gradients to compute anomaly source location [5].

Aeromagnetic techniques were also used for depth to magnetic origins in Nigeria's Nupe Basin. In the study area, the three sedimentary formations discovered include sandstone facies, claystone facies, and ooidal ironstones [6]. Source parameter imaging (SPI) was employed in estimating the depth to magnetic sources from the observed total magnetic field intensity. The SPI was computed using the AS amplitude, local frequency, and phase [6]. Onyishi and Ugwu *et al.* used Oasis Montaj and PotentQ software tools to compare the depth to magnetic source in the Benue Trough, Nigeria, using both Euler deconvolution and SPI techniques [7]. The investigations revealed that there was better agreement at deep depths (SPI: 4409.5 m and Euler: 4909.3 m) than at shallow depths (SPI: 318.7 m and Euler: 902.3 m). It was, however, useful to combine other geophysical survey methods to determine the formations, as shown in refs [7,8] in an analysis of groundwater assessment in the coastal plain of southwest Nigeria. Joel *et al.* combined electrical resistivity imaging with the aeromagnetic technique to map the hydrogeological structure. The depth of the magnetic source was also determined using SPI. The majority of the authors used Geosoft Oasis Montaj commercial software tools to delineate edges of buried magnetic bodies and compute sedimentary thickness from their aeromagnetic data. Some of the tools in this software were applied to the investigation of deep magnetic sources identified in sedimentary terrains [9] to identify long-wavelength signatures on the TMI, while noise or shallow magnetic sources were identified by short-wavelength signatures. AS has been used to delineate the edges of iron ore bodies, near low magnetic latitude, which occasionally renders map analysis more complicated. The magnetic SPI depth estimates were determined ranging from 20 to 100 m near the surface [9].

The functionalities of popular commercial software applications can restrict the options of the aeromagnetic data processing system. The Signum transformation method is a one-of-a-kind depth estimation method that has yet to be widely published. The Signum transformation algorithm classifies linear image patterns in potential fields, identifying the signal's positive element and calculating pattern width by finding the largest graved circles in the region where the signal is positive [10]. The short processing time and analogy to the findings of the Euler deconvolution demonstrated the algorithm's usefulness in the interpretation of magnetic anomalies. The algorithm was tested on magnetic data, where the crossover points had physical meaning; however, it may be useful in any interpretation approach that necessitates the automated calculation of contour data distance [10].

Automatic characterization of sedimentary basin and its surrounding basement was demonstrated using amplitude-normalized return to the pole (RTP) magnetic data to improve edge detection; a tilt-angle filter was applied to the RTP aeromagnetic survey data [11]. Other approaches for structural characterization of sedimentary basins and lineaments that have been widely published are discussed. The findings show how gridded aeromagnetic-field data can yield geologically viable results that can be used to constrain the architecture of basins containing magnetic sedimentary rocks.

2 General principle of finding buried materials

Sedimentary strata juxtaposed around faults would show anomalies to predict the existence of faults that are deduced by physical variation in magnetic susceptibility, dip, thickness, and depth of the strata [12]. Aeromagnetic contour maps could show some linear anomalies in subsurface mapping. These contour maps help to connect fault surfaces and clarify the presence of undefined fault surfaces. It is worth understanding that magnetized sedimentary layers in physical terms vary from layers of magnetic contrast. A sedimentary magnetized stratum has a susceptibility value that is equivalent to the amount of magnetic minerals present in the sediment layers [13]. Furthermore, the sedimentary stratum from which the susceptibility values are extracted has a direct physical analogy in geology. The magnetic contrast layer is derived by calculating the positive contribution in susceptibility between the formation of two magnetic layers positioned side by side around a fault and assigning the resulting value to the layer with higher magnetic susceptibility.

The Earth's magnetic field strength is affected by the distribution of magnetic materials within it [14]. The International Geomagnetic Reference Field (IGRF) models are meant to predict the expected value of the magnetic field of Earth's that is of internal origin for an epoch period of five years [15]. Magnetic anomaly results from a comparative difference between the measured Earth's magnetic field amplitude and the value expected at that position:

$$\text{Magnetic anomaly (MA)} = \text{Measured value (MV)} - \text{Expected value (EV)}$$

The direction of magnetization is generally affected in magnetic anomalies, making it difficult to use the raw magnetic anomaly data to determine accurately the precise location or geometry [14].

The current version, the 13th generation IGRF-model's Gaussian coefficients, represents the low-order terms that model magnetic field originating from within the core, using spherical harmonics [16]. When supplied with geodetic coordinates of latitude, longitude, and altitude on a specific date, it calculates expected values of declination, inclination, north intensity, east intensity, horizontal intensity, vertical intensity, and total intensity for both the main field and secular variation [17]. The models used a simplified approach and accept vertical magnetization and zero declination. The Earth's magnetic field includes short-wavelength components caused by magnetic materials of exploration interest within the Earth's crust and long-wavelength components caused by metallic geo-dynamo in the Earth's core, both of which are time varying [14,18].

3 Aeromagnetic expression of intra-sedimentary faults

Sedimentary strata are defined as magnetized uniform deposits of finite thickness that extend laterally to infinity in geophysical models. However, for geographic horizontal layers, no matter how strong, the magnetic susceptibility cannot cause an anomaly. High magnetic susceptibility alone cannot guarantee that an anomaly will exist. The key geophysical features that determine the presence of anomaly at fault were explained in ref. [19]. If two such layers with different magnetic susceptibilities are placed next to each other and truncated at a fault toward each other, an anomaly will be generated by the lateral magnetic contrast at the juxtaposition boundary [20]. The lateral magnetic contrast of the layer, the vertical amplitude, juxtaposed boundary dip, magnetometer observation height above and depth below the ground will all influence the geophysical value of the anomaly.

In regional aeromagnetic surveys, rocks and sediments within sedimentary basins were typically considered nonmagnetic; however, as more high-resolution aeromagnetic surveys are flown at low altitudes and with close line spacing, subtle magnetic anomalies are increasingly being discovered. Modern magnetometers can sample every 5 m, meaning it will cycle once every 0.1 s on the field with a resolution of 0.001 nT. Position errors of less than 2 nT can be achieved with real-time differential GPS data and preprogrammed flight lines to increase the spatial precision in a horizontal position to around 2–3 and 15 m in vertical position. Low-amplitude and short-wavelength magnetic anomalies can be resolved by using survey designs with close line spacing (<250 m) and low flight elevations (350 m) stretched over the field [21]. As proposed by Gunn *et al.* [22], close line spacing (400 m) and the use of precision instrumentation would highlight the relatively small-amplitude anomalies produced by shallow magnetized sources. Low flight-heights are recommended to detect accurately the magnetic source and more coherent anomalies. Data analysis and processing undertaken would suppress heavy regional gradients and differentiate the slight sediment-produced anomalies from the noticeably extreme basement characteristics.

The hypothetical relationship between the magnetic anomaly and its associated geology was demonstrated using a stratigraphic geological model and its corresponding geophysical model, which were designed to complement each other [20]. The basic magnetic-contrast layer model signatures associated with intra-sedimentary faults of four major types were well described. The layers with no magnetic contrast simply stretched through fault line without delineation, despite the fact that fault truncated all layer forms.

The general challenge is to find a way to delineate edges with little or no knowledge about the underlying magnetic-contrast layer structure. Derivative functions are commonly used to find edges in aeromagnetic data [23]. It is based on the behavioral characteristics of the magnetic field over an ideal, near-vertical, finite, or infinite thickness layer. The reduction to magnetic anomalies is equivalent to relocating an anomaly to the North Pole, transforming them to what they would look like if the anomalies causing bodies were vertically magnetized. Reduction or RTP was used to improve aeromagnetic data over north-central Nigeria. The RTP adjustment improved the placement of the anomaly peaks over the source to reveal the sedimentary thickness of less than 1 km [24]. The magnetic anomalies are also converted or reduced to pseudo gravity anomalies. Both data reductions are accomplished efficiently by converting field observed data to its frequency domain and applying sufficient filters with terms containing values for inclination angles, ambient magnetic field declination, and the magnetization of the bodies causing anomalies [18].

Another way to delineate edges that are perfectly suitable for aeromagnetic data is the horizontal gradient technique [20]. The local horizontal gradient magnitude (HGM) and maxima of RTP potential field data are used to estimate the steepest gradient that is correlated with near-vertical boundaries [25]. The benefits of the horizontal derivative approach compared with other approaches based on derivatives are consistency in the presence of noise and its fast grid adaptation without the need for additional parameter modification [26].

Longitudinal anomalies are caused by faults in sedimentary basins due to tectonic juxtaposition, serendipitous exposure, or variation in magnetic characteristics along the fault plane [27,20]. We aim to understand better the relationship, particularly:

- What is needed to create an aeromagnetic anomaly from a fault
- How to detect a trace of a hidden fault from an anomaly
- Assessment of fault geometry and displacement from an anomaly
- The amount of anomaly attributed to topography.

Grauch and Hudson. examined the association between aeromagnetic signatures of fault geometry, juxtaposed strata, and magnetic features to variations [20]. The basic signatures associated with intra-sedimentary faults describing four major model types of the magnetic-contrast layer are the following:

1) The truncated-layer structure is defined by only a single layer that is truncated at fault.
2) The offset layer structure is made up of two offset layers with equal magnetic susceptibility and thickness.
3) Two offset layers of similar thickness but differing magnetic susceptibility represent the contrasting-layer structural model.
4) Two offset layers with a much thicker upper layer but the same magnetic susceptibility represent the thin-thick layer model structure.

The magnetic susceptibility contrast Δm as shown in Figure 1 at a specific depth d and the corresponding thickness t to a given amplitude of anomaly T_{anom} at observation height of h is given by equation (1):

$$\Delta m = \frac{\pi T_{\text{anom}}}{F_0}\left[\tan^{-1}\sqrt{\frac{d+h+t}{d+h}} - \cot^{-1}\sqrt{\frac{d+h+t}{d+h}}\right]^{-1}, \quad (1)$$

where $T_{\text{anom}} = T_{\max} - T_{\min}$.

At a certain depth d, T_{anom} can be updated using equation (2) by simply multiplying the ratio of the

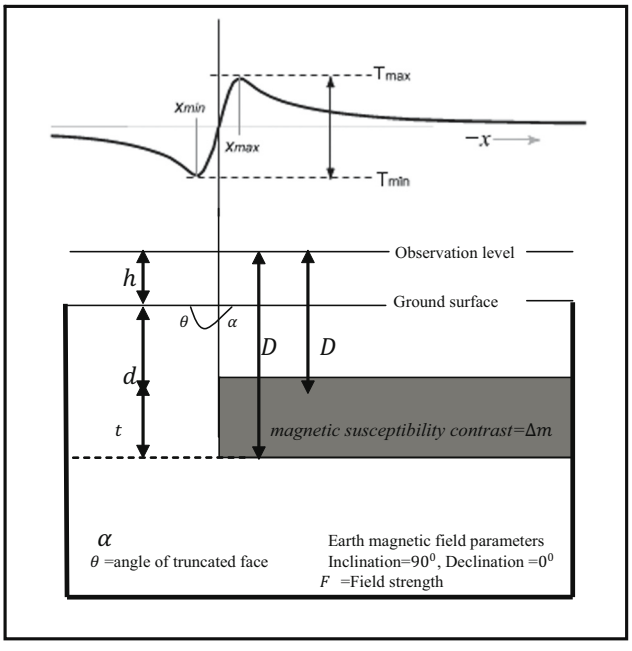

Figure 1: Single truncated layer model adapted from ref. [20].

magnetic-contrast Δm by the new value's proportion new T_{anom} in relation to the previous one, T_{anom}.

$$\text{New } \Delta m = \Delta m \times \frac{\text{New } T_{\text{anom}}}{T_{\text{anom}}}. \quad (2)$$

For the magnetic contrast layer at depth d with its fault dipping at an angle α as observed from height h, the maximum lateral offset l_{offset} of the HGM from fault trace is given by equation (3):

$$l_{\text{offset}} = \begin{cases} 0; \text{ for } \alpha = 90°, \\ d(\cot \alpha + f_{\propto}) + hf_{\propto}; \quad \text{for } 0° < \alpha < 90°, \end{cases} \quad (3)$$

$$f_{\propto} = \left| \frac{1 - \sin \propto}{\cos \propto} \right|.$$

The following guidelines were deduced:

- the anomaly would not be observed (even if fault throw is >500 m) if the disparity between juxtaposed layers of magnet susceptibility is less than 0.2×10^{-3} (SI),
- the anomaly would not be observed if fault throw is below 10 m (even with magnetic susceptibility contrast up to 3.0×10^{-3} (SI)),
- the aeromagnetic anomaly can be detected for faults projecting more than 30 m to the surface, and
- if the first top magnetic contrasts layer depth is between 100 and 300 m, faults will need up to 50–100 m for the throw to be detected.

The use of the thickness contrast needs three significant notes:

(1) The graph should not be used to measure the magnetic contrast depth of magnetic anomaly. The conventional geophysical methods calculate depth by the shape of an anomaly rather than its magnitude [20]. Deep magnetic contrasts produce broad anomalies, while shallow magnetic contrasts produce sharp and small anomalies because the magnitude of such an anomaly caused by certain magnetic contrast is measured by depth.
(2) The thickness of the layer should not be equated with fault without sufficient magnetic susceptibility and stratigraphy information.
(3) All local landscapes and stratigraphic layers juxtaposed with the fault should be taken into account when estimating magnetic contrasts using field calculation. The use of the horizontal derivative technique to RTP data often must deal in practice with the issue of regional magnetic gradients superimposed, which modify the structure of the local aeromagnetic signature. Prior to computing the HGM, the horizontal gradient window technique should be used to eliminate the regional trend from such a sliding window of data.

4 Depth estimation using Euler deconvolution

The Euler deconvolution is window-based, widely used for magnetic problems to determine depth estimates along a potential field profile. Its normal Cartesian implementation is expressed in equation (4):

$$(x - x_0)\frac{\partial T}{\partial x} + (y - y_0)\frac{\partial T}{\partial y} + (z - z_0)\frac{\partial T}{\partial z} = N(B - T), \quad (4)$$

where (x_0, y_0, z_0) refers to the position of the source, whose total field T is detected at (x, y, z) and B is the potential field's regional value.

To maintain its geological relevance, it is important to ensure that parameters like SI are correctly chosen. The following principles for design consideration are based partly on the mathematical theory and partly on practice. A simple structure with an integer magnetic SI (Table 1) suitable for the geology and geophysical interpretation problem of the buried source must be assumed [28,29].

The solution for each window location is limited to resolving the potential field effect of a single isolated edge of one restricted range of the SI model [29,30]. The following are multisource solutions developed to accommodate the impact of various sources on each window:

(1) The SI for each anomaly can be indirectly calculated by optimizing the SI value that results in the lowest local disruption of the computed background value, B. We should not see the SI as a parameter for tuning because it has its own geological significance of source shape. Magnetic SI values that are too high create exaggerated depths and *vice versa*. It is also

Table 1: SI value of the basic magnetic field model

SI value	Type of a magnetic model
3	Point and spherical sources
2	Vertical and horizontal cylinders, thin-bed fault, line
1	Sills and dyke, a thin prism with large circles
0.5	Contact with a small depth extent
0	Thick sheet edge

important that there should be a structural edge at any one (x, y) spot, such that a single depth solution has some significance [31].

(2) The area should be correctly sampled without substantial aliases. If the interval (for example, flight lines) is too spaced, high-amplitude field data of shorter wavelength would not be observed. Moreover, fine interpolation or over-gridding does not add details to the maps. The grid interval must match both the problem and data without having to over-grid or sparingly grid the relevant information. The interval of the grid should be as wide as possible in order to better represent the area.

(3) Check whether your gradient information (calculated or measured) is sufficiently noise-free and represents the gradient of primary data. The gradients are calculated by empirical methods. While it is possible to quantify horizontal gradients using finite difference or splines, vertical derivatives usually involve Fourier processes. Measurement of the horizontal derivative must comply with minimal aliases and minimal noise requirements.

(4) Window size of the deconvolution would need to be at minimum twice as wide as the actual grid spacing for grid data, alternatively for line spacing. It should also be greater than half the depth of the investigated source. Depths above twice the window dimension are furthermore unstable [29]. The "thumb rule" for the actual size of the window is, therefore:
   (a) Smallest possible width
   (b) More than double the interval of assessed line or grid data
   (c) More than half the investigative depth required.

(5) The always present scattering of false solutions must be minimized, identified/discarded, and overlooked by diligent application of clustering parameters and its reliability criteria. Almost every Euler devolution algorithm implementation produces sprays of so-called "false results," which are attributed to a number of reasons, including interaction with nearby sources, by sources laterally distanced from the window. The Euler deconvolution algorithm involves ways of minimizing the number of such bogus solutions.

(6) If the program involves an Euler deconvolution algorithm in Cartesian form (more commonly accessible), the procedure must be implemented using Cartesian coordinates [29]. Expansion in Fourier occurs naturally by the separation of variables in the Cartesian space to solve possible field problems. The gradients derived from the Fourier equation, if applied with data represented in geographical coordinate would generate the invalid and deceptive result. Any geographical data should be re-projected to the Cartesian space before computing the Fourier gradient, or carrying out any Euler deconvolution using standard implementation so to eliminate distortions and misleading results.

5 Depth estimation/edge detection using the Signum approach

Some of the shortcomings of the Euler deconvolution technique can be improved upon by using the ST discussed in this section [32]. The ST method can locate spatial irregularities that can be used to measure the causative source depth and width. First, the magnetic anomaly is improved using a simple edge filter transform, which only maintains signs of irregular fields [10]. The theoretical edge position will be referred to as the points at which one derivative of the perceptual fields (or their functions) changes sign. The Signum-transformed spatial derivatives help to quickly define those points. The true source depth and width of the positive plateaus are then measured using two separate data converted by the Signum: One is based on the vertical derived while the other is determined by subtracting the absolute value of the horizontal gradient from the vertical gradient [10]. The largest circle radius within positive plateaus was computed using the automated algorithm. Numerical testing with synthetic data demonstrated that accurate predictions for target parameters are given by the Signum method. The vertical dyke model observed at the magnetic pole $z = 0$ will present a magnetic anomaly given as

$$M = A\left(\tan^{-1}\frac{x+a}{h} - \tan^{-1}\frac{x-a}{h}\right), \tag{5}$$

where A is the amplitude coefficient, a is half the width of the dike, and h is depth to the dike's top.

For any magnetic anomaly M, which could be the first- or second-order vertical gradient or subtracting the total horizontal gradient from the first-order vertical gradient [33] as expressed in equation (5), the zeros should ideally be at $\pm a$;

$$\frac{\partial M}{\partial z} = 0, \quad \frac{\partial M^2}{\partial z^2} = 0, \quad \frac{\partial M}{\partial z} - \left|\frac{\partial M}{\partial x}\right| = 0. \tag{6}$$

Solving equation (6) for x provides the zero-crossover points for all three functions.

For the first-order vertical gradient function, the zero crossover point is given as

$$x_v = \pm\sqrt{a^2 + h^2}. \tag{7a}$$

The zero crossover point for the second-order vertical gradient function is given as

$$x_{vv} = \frac{\sqrt{3}}{3}\sqrt{2(a^4 + a^2h^2 + h^4)^{1/2} + a^2 - h^2}. \tag{7b}$$

The zero crossover point for the first-order vertical gradient minus the total horizontal gradient function is

$$x_{vh} = \pm h - \sqrt{a^2 + 2h^2}. \tag{7c}$$

Equations (7a–c) revealed that the deeper the dike depth "h," the more the zero-crossover point would shift from the true edge location. As h tends to zero, all the three zero-crossover points expressed in equation (7a–c) converge to $\pm a$. The Signum function provides an easy way to locate the zeros (of equation (6)) and can be expressed as in equation (8) for which $k = 0$ corresponds to a well-known sign function

$$\mathrm{ST}[f] = \begin{cases} \dfrac{f}{|f|}, & f \neq 0, \\ k, & f = 0. \end{cases} \tag{8}$$

The ST has just two values, –1 or +1, and the theoretical edges correspond to the point where the sign changes values giving some advantage over other derivative-based edge detection methods that sort for peaks in the transformed anomalies.

Combining equations (7a) and (7c) result to dike depth "h" and edge formulae "a" gives:

$$h = \frac{x_v^2 - x_{vh}^2}{2x_{vh}}, \tag{9}$$

$$a = \sqrt{x_v^2 + h^2}. \tag{10}$$

The input parameters for equations (8) and (9) can be derived from two Signum-transformed anomalies from two anomaly maps.

If the ST of two derivatives, namely the first and second derivatives are overlaid, the resulting colors of the map can be used to resolve magnetic sources that are in very close neighborhoods. The ST equates to unity for any function as expressed in equation (8). Different colors are used to represent the unity values for the functions as illustrated in Figure 2. Lighter blue depicts the region on the map where ST of the first derivative equates to unity. The orange color depicts unity value regions of the second-derivative ST. The region where both the light blue and orange color overlaps and both functions equate to unity is represented with the red-colored region.

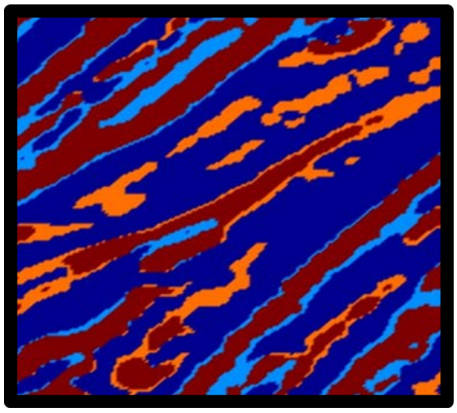

Figure 2: An illustration of the ST's ability to separate closely spaced magnetic sources modified after ref. [33].

6 Discussion

Aeromagnetic anomaly data can be obtained and displayed as maps for which optimal portrayal of geological detail such as anomaly can be deduced. This article contributes toward synthesizing the information that can be used as a reference for analyzing the use of certain methods in order to minimize any misconceptions or deceptive geophysical views of results. The use of magnetized sedimentary strata was discussed. The magnetized strata that have susceptibility values that are equivalent to the amount of magnetic minerals had also been compared with the magnetic contrast layer. This comparison was used to justify the relationship between both the magnetic anomaly with its related geology and the stratigraphic-based model with its equivalent geophysical model.

As compared to other observable variables resulting from methods based on derivatives, the horizontal gradient approach using maxima of RTP magnetic data to delineate edges has the advantages of accuracy in the presence of noise and rapid grid adaptation without the need for additional parameters' adjustment. Generally, the effect of the variable is determined by the quality of the data and how it would be processed. Some observed variables are more difficult to predict and may appear like nearby anomalies. They could be seen as interference that could create offsets. The nonplanar regional disturbance may result in similar interference. The Terrain

effect over the observational surface and the grid interval may also limit the resolution of detecting detailed features on the map. Some sharp corners of three-dimensional geological structures or abnormal or gradational boundaries that cannot be resolved can also be present as interference. If the scale of the sample region shrinks, all of these considerations become more important and the small quantities of offset they create become more apparent.

The criteria for the aeromagnetic anomaly to be visible and hidden fault detected were addressed and the method on how to assess the geometry and displacement of a fault from an anomaly was considered. To maintain geological relevance, parameters like the choice of SI and other principles for design considerations based on theory and partly on practice were discussed. In order to preserve geological relevance, criteria such as SI selection and other design concepts based partly on the theory experience of writers were discussed. However, some of the shortcomings of Euler deconvolution techniques were improved upon using the ST. The positive plateau depth and width from the source were calculated using the vertical derivative as well as the vertical derivative minus the absolute value of the horizontal derivative [10]. An advanced algorithm was used to calculate the radius of the largest circle contained within the positive plateaus. The Signum method provided accurate predictions for the target parameters when evaluated with synthetic data.

7 Conclusion

Data processing techniques are important to procedures leading to geological models and interpretation of anomaly maps. Without any information about depth, spread, lateral extension, and vertical extension of underlying bodies, it is considered to adopt several data processing techniques in analyzing the general parameters that could help to understand the nature of the causative body. However, using both the Signum method and Euler deconvolution techniques would improve representations and greater precision can be obtained, eliminating the nonuniqueness of the outcomes in the reverse problem solution.

Funding information: The authors appreciate Covenant University Centre for Research Innovation and Discovery (CUCRID) and Covenant University as a whole for their financial support towards this study.

Author contributions: B.H.O. supervised this research and also project administration. A.P.A. edited the paper. O.O.A. conceptualized the formal analysis, wrote the original draft, and edited the paper. All authors have accepted responsibility for the entire content of this manuscript and approved its submission.

Conflict of interest: The authors state no conflict of interest.

Data availability statement: Data sharing is not applicable to this article as no datasets were generated or analysed during the current study.

References

[1] Innocent AJ, Chidubem EO, Chibuzor NA. Analysis of aeromagnetic anomalies and structural lineaments for mineral and hydrocarbon exploration in Ikom and its environs southeastern Nigeria. Jour Afr Earth Sci. 2019;151:274–85.

[2] Ambrosino F, Thinova L, Briestensky M, Sabbarese C. Anomalies identification of Earth's rotation rate time series (2012–2017) for possible correlation with strong earthquakes occurrence. Goedesy Goeodynamic. 2019;10(6):455–9.

[3] Caracciolo FA, Nicolosi I, Carluccio R, Chiappini S, De Ritis R, Giuntini A, et al. High resolution aeromagnetic anomaly map of Mount Etna volcano, Southern Italy. J Volcanol Geotherm Res. 2014;277:36–40.

[4] Abubakar Nda'asabe D, Yusuf Abubakar S, Muhammad SB, Salako AK. Euler deconvolution and two-dimensional modelling of subsurface structures over part of northern Bida basin and its surrounding basement rocks, northwest, Nigeria using magnetic method. Int J Earth Sci Geophy. 2020;6(2):1–11. doi: 10.35840/2631-5033/1838. (ISSN: 2631-5033).

[5] Osinowo OO, Taiwo TO. Analysis of high-resolution aeromagnetic (HRAM) data of Lower Benue Trough, South-eastern Nigeria, for hydrocarbon potential evaluation. NRIAG J Astron Geophys. 2020;9(1):350–61. doi: 10.1080/20909977.2020.1746890.

[6] Opeloye SA, Amigun JO, Sanusi SO, Alabi O. Palaeoenvironmental reconstruction and oolitic ironstone mapping of the Agbaja Ironstone formation in the Nupe Basin, North-central Nigeria: insights from sedimentological and aeromagnetic analyses. Results Geophys Sci. 2021;5:100010.

[7] Onyishi GE, Ugwu GZ. Source parameter imaging and Euler deconvolution of aeromagnetic anomalies over parts of the middle Benue trough, Nigeria. Am J Geophys Geochem Geosyst. 2019;5(1):1–9.

[8] Joel ES, Olasehinde PI, Adagunodo TA, Omeje M, Akinyemi ML, Ojo JS. Integration of aeromagnetic and electrical resistivity imaging for groundwater potential assessments of coastal plain sands area of Ado-Odo/Ota in southwest Nigeria. Groundw Sustain Dev. 2019;9:100264.

[9] Adejuwon BB, Ibeneme SI, Osizemete AG, Obioha YE, Abba AU. Quality assessment and reserve estimation of the egnaeja iron ore deposit, north-central Nigeria using integrated approach. Int J Earth Sci Geophs. 2020;6(2):1–12. doi: 10.35840/2631-5033/1837. (ISSN: 2631-5033).
[10] Oliveira SP, Ferreira FJ, de Souza J. EdgeDetectPFI: an algorithm for automatic edge detection in potential field anomaly images–application to dike-like magnetic structures. Comp Geosci. 2017;103:80–91.
[11] Nathan D, Aitken A, Holden EJ, Wong J. Imaging sedimentary basins from high-resolution aeromagnetic and texture analysis. Comp Geosci. 2019;136:104396. doi: 10.1016/j.cageo.2019.104396.
[12] Rao DA, Babu HVR. Standard curves for the interpretation of magnetic anomalies over vertical faults. Geophys Res Bull. 1983;21:71–89.
[13] Hudson MR, Grauch VJS, Minor SA. Rock magnetic characterization of faulted sediments with associated magnetic anomalies in the Albuquerque basin, Rio Grande Rift, New Mexico. Geol Soc Am Bull. 2008;120(5–6):641–58. doi: 10.1130/B26213.1.
[14] Hulot G, Sabaka TJ, Olsen N, Fournier A. The present and future geomagnetic field. Treatise Geophys. 2015;5:33–78. doi: 10.1016/b978-0-444-53802-4.00096-8.
[15] Yang Y, Hulot G, Vigneron P, Shen X, Zhima Z, Zhou B, et al. The CSES global geomagnetic field model (CGGM): an IGRF-type global geomagnetic field model based on data from the China Seismo-Electromagnetic satellite. Earth, planets space. 2021;73(1):1–21.
[16] Thébault E, Finlay CC, Beggan CD, Alken P, Aubert J, Barrois O, et al. International geomagnetic reference field: the 12th generation. Earth Planets Space. 2015;67(1):1–9. doi: 10.1186/s40623-015-0228-9.
[17] Li Y, Nabighian M. Tools and techniques: magnetic methods of exploration – principles and algorithms. Treatise Geophys. 2015;3:335–91. doi: 10.1016/b978-0-444-53802-4.00196-2.
[18] Talwani M, Kessinger W. Encyclopedia of physical science and technology. (Third edn). Texas, USA: Academic press, Rice University Houston; 2003.
[19] Blakely RJ. Potential theory in gravity and magnetic applications. USA: Cambridge University Press; 1995.
[20] Grauch VJS, Hudson MR. Guides to understanding the aeromagnetic expression of faults in sedimentary basins: lessons learned from the central Rio Grande rift, New Mexico. Geosphere. 2007;3(6):596–623.
[21] Liang S, Sun S, Lu H. Application of airborne electromagnetics and magnetics for mineral exploration in the Baishiquan–Hongliujing area, northwest China. Remote Sens. 2021;13(5):903. doi: 10.3390/rs13050903.
[22] Gunn PJ, Maidment D, Milligan PR. Interpreting aeromagneic data in areas oflimited outcrops. Jour Aust Geol Geophy. 1997;17(2):175–85.
[23] Marr D, Hildreth E. Theory of edge detection. Proc R Boc Lond B. 1980;207:187–217.
[24] Irumhe PE, Obiadi II, Obiadi CM, Ezenwaka CK, Mgbolu CC. Estimating sedimentary pile thickness, structural lineaments and heat flow in parts of North Central Nigeria from aeromagnetic data. Solid Earth Sci. 2019;4(3):92–101. doi: 10.1016/j.sesci.2019.06.001.
[25] De Souza J, Ferreira FJF. On the use of derivatives for interpreting magnetic anomalies due to dyke-like bodies II: application to synthetic and field data. SEG Houston 2013 Annual Meeting. Society of Exploration Geophys; 2013.
[26] De Souza J, Ferreira FJF. On the use of derivatives for interpreting magnetic anomalies due to dyke – like bodies: qualitative and quantitative analysis. Istanbul – 2012 International Geophysical Conference and Oil & Gas Exhibition, SEG; 2012.
[27] Grauch VJS, Hudson MR, Minor SA, Caine JS. Sources of a long-strike variation in magnetic anomalies related to intrasedimentary faults: a case study from the Rio Grande Rift, USA. Expl. Geophy. 2006;37(4):372–8. doi: 10.1071/EG06372.
[28] Stavrev P, Reid A. Degrees of homogeneity of potential fields and structural indices of Euler deconvolution. Geophys. 2007;2:L1–L12.
[29] Reid AB, Ebbing J, Webb SJ. Avoidable Euler errors–the use and abuse of Euler deconvolution applied to potential fields. Geophys Prospect. 2014;62(5):1162–8.
[30] Ravat D. Analysis of the Euler method and its applicability in environmental investigations. J Env Eng Geophys. 1996;1:229–38.
[31] Webb SJ. The use of potential field and seismological data to analyze the structure of the lithosphere beneath southern Africa. Ph.D. thesis. Johannesburg: University of the Witwatersrand; 2009.
[32] Weihermann JD, Ferreira FJF, Oliveira SP, Cury LF, de Souza J. Magnetic interpretation of the Paranagua Terrane, southern Brazil by signum transform. Jour Appl Geophys. 2018;154:116–27.
[33] De Souza J, Ferreira FJ. The application of the Signum transform to the interpretation of magnetic anomalies due to prismatic bodies. ASEG Ext Abstr. 2015;2015(1):1–5.